

A Lattice Gas Approach to the Mexico City Wind Field Estimation Problem

Alejandro Salcido and Ana Teresa Celada Murillo
*Instituto de Investigaciones Eléctricas, División de Energías Alternas
México*

1. Introduction

Although in 1992 the United Nations Environment Programme and the World Health Organization included Mexico City among the megacities with the worst air pollution problems (UNEP & WHO, 1992), the environmental actions carried out by the local governments of the Mexico City Metropolitan Area (MCMA) in the following fifteen years, particularly in the period 2000-2006, produced very important reductions in the emissions of air pollutants. Emission reductions around 86% in sulphur dioxide (SO₂), 60% in carbon monoxide (CO), 30% in nitrogen oxides (NO_x), 50% in PM₁₀ (particulate matter < 10 μm in diameter), and 40% in volatile organic compounds (VOC), were reported for the years 1990-2006 in the official emission inventory (SMA-GDF, 2008). Nevertheless, nowadays, close to 1.8 megatons of CO, 187 kilotons of NO_x, 6 kilotons of SO₂, 21 kilotons of PM₁₀, and 512 kilotons of VOC are still being produced in the MCMA and released to its ambient atmosphere every year (SMA-GDF, 2008). The critical air pollutants in MCMA are ozone (O₃), PM₁₀ and PM_{2.5} with concentrations above their daily and annual US air quality standards (Bravo & Torres, 2002). Ozone, however, is by far the most important air pollutant because of the frequency of occurrence of high levels, persistence, and spatial distribution (Bravo & Torres, 2002; Bonner et al., 1998; Osornio-Vargas et al., 2006).

Besides the emissions, however, other very important factors, such as the geographical setting, the topography, the meteorology, and the properties of the urban surface, and their possible interactions, must be taken into account in the analyses to understand properly the complexity and gravity of the MCMA air pollution problem. The MCMA is situated inside a subtropical basin (19.0-20.0 °N, 98.5-99.5 °W) which extends over an area of 60 x 60 km², approximately, and has an average altitude of 2240 m. As it is shown in Figure 1, the MCMA is surrounded by high mountains on three sides: west, south and east. To the west and south are the *Sierra Las Cruces* and the *Sierra Ajusco-Chichinautzin* (which its highest point is the peak *Cruz del Marques* in the volcano *Ajusco*, with an altitude of 3937 m). To the east, starting with the *Sierra Santa Catarina*, there is a north-south barrier consisting of three peaks, with the volcanoes *Iztaccihuatl* and *Popocatepetl* reaching elevations of 5222 and 5465 meters above sea level (masl), respectively. At the southeast corner of the MCMA basin the terrain falls, creating a low-lying gap through the mountains. To the north, the basin extends into the Mexican plateau and the arid interior of the country, with the *Sierra de Guadalupe* creating a

small 800 m barrier above the basin floor. Its climate, otherwise, is usually classified into two seasons: the rainy season from May to October, and the dry season from November to April. This classification stems from the two main meteorological patterns on the synoptic scale: dry westerly winds with anticyclonic conditions from November until April, and moist flows from the East due to the weaker trade winds along the other six months. Very often, however, the meteorology at the MCMA is more complex than this simple classification. Important interactions of the basin with the Mexican plateau and the lower coastal areas may occur. Moreover, due to the MCMA location, large-scale pressure gradients are generally weak, and a very strong solar radiation is registered there throughout the year. In 2001, the MCMA global solar radiation ranged 150-300 W/m² in average, with maximum values from 800 to 1100 W/m²; and wind speeds from 2 to 3 m/s were observed at urban sites, and from 3 to 4 m/s in suburban areas, in average (Salcido et al, 2003a). These conditions, combined with the surrounding mountains, are ideal for the development of thermally driven winds, including upslope, downslope, and heat island winds.

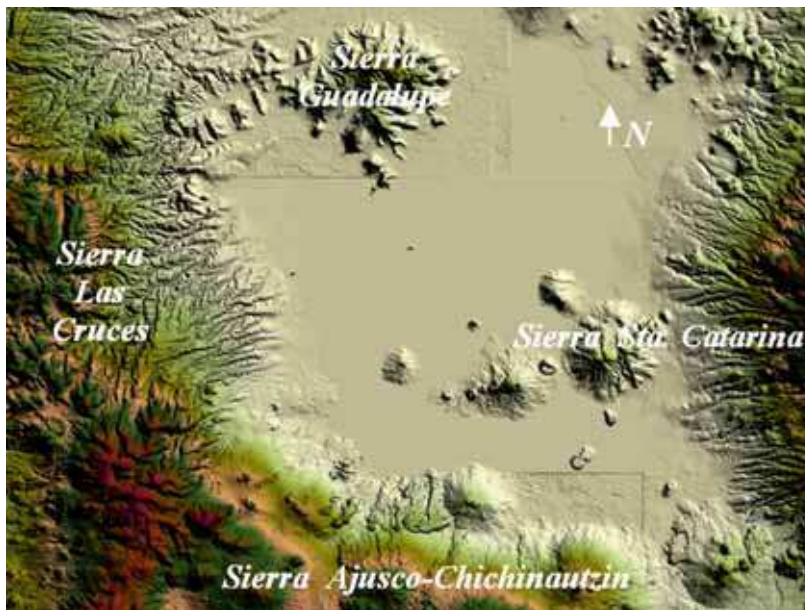


Fig. 1. Main topographic features of the Mexico City Metropolitan Area

The knowledge of the wind circulation events and their possible organization in patterns constitute an important issue to understand how the emissions of air pollutants may be dispersed in an urban settlement and how its air pollution may be exported towards the neighboring sites. Although the MCMA is surrounded by high mountains and it may lead to the trapping of air pollution up to for several days, it is also frequent that the mixing height may reach values higher than 2600 m above ground level (Salcido et al, 2003b), and these conditions favor exportation of air pollution from the MCMA to its surroundings (Castro & Salcido, 2006). On another hand, because the changes in the urban design and the spatial distribution of the built can affect the surface wind circulation in the cities, the short

and long term evolution of the urban wind patterns are relevant also for urban bioclimatic studies. Nowadays, this is also a particularly important issue in relation with the MCMA air pollution problem because in the last seven years the urban morphology was changed significantly by the construction of a second traffic floor above the Periferico freeway (a primary via which surrounds the city from north to south) and by an explosive growing of the number of the skyscrapers and other big buildings in the city. These all are wind field applications that belong to the meso- γ scale or turbulence scale meteorology problems.

The theoretical basis of meteorology is in the Navier -Stokes equations, which constitute a system of coupled and non-linear partial differential equations. For small velocities, these equations can be linearised and solved without much difficulty, analytically if the solid boundaries involved are simple, and numerically otherwise. However, when air flow velocities are large, instabilities may appear and exact analytical methods can no longer be used. Even numerical methods are difficult to use, chiefly because scales of different sizes must be taken into account, which forces grids either to be very small or variable.

In practice, a lot of powerful computer simulation tools for diagnostic and prognostic purposes, ordinarily known as meteorological models, have been developed (and still are being developed) to find out the wind fields and other meteorological variables for a variety of applications. A diagnostic model simply provides an estimate of a steady state condition because it contains no time-tendency terms, includes little physics in its calculations and provides meteorological fields derived by appropriate interpolation and extrapolation of available data. A prognostic model, instead, does incorporate meteorology physics and can be used to forecast the space-time evolution of the system by numerical integration of time-dependent differential equations. However, the numerical solutions depend strongly on boundary conditions and initial values; so that special care must be taken to correctly initialise all meteorological variables in the computational domain and to correctly define the time-varying physics at the boundaries. Two excellent prognostic meteorological models are the PSU/NCAR mesoscale model (known as MM5) and the Weather Research and Forecasting (WRF) model. These two models are complex and heavy numerical simulation instruments adequate only for mesoscale meteorology problems (MM5, 2003).

A quite different strategy to simulate fluid behaviour has been developed in the last two decades using the cellular automata techniques introduced by John von Neumann and Stanislaw Ulam in the early 1950s (von Neumann, 1966). Fully discrete models obeying cellular automata rules have been developed for the microscopic motion of the particles of a gas, such that the coarse-grained behaviour (in the thermodynamic limit) lies in the same universality class as the fluid flow phenomenon. This class of dynamical systems, known as lattice gas models, consist of a regular lattice, each site of which can have a finite number of states representing the directions of motion of the gas particles, and evolves in discrete time steps obeying a set of homogeneous local rules which define the system dynamics. These rules must be defined in such a way that the physical laws of conservation of mass, momentum and energy are fulfilled during the propagation and collisions of the gas particles (Boghosian, 1999). Typically, only the nearest neighbours are involved in the updating of any lattice site.

The first attempt along these lines was undertaken by Leo P. Kadanoff and Jack Swift in 1968 (Kadanoff & Swift, 1968). The Kadanoff-Swift model exhibits many features of real fluids, such as sound-wave propagation, and long-time tails in velocity autocorrelation functions. As the authors noted, however, it does not faithfully reproduce the correct motion

of a viscous fluid (Boghosian, 1999). The next advance in the lattice modelling of fluids came in the mid 1970's, when J. Hardy, O. de Pazzis and Y. Pomeau introduced a new lattice model (the HPP model, named for its authors) with a number of innovations that warrant discussion here (Hardy et al, 1973; Hardy et al., 1976). Like the Kadanoff-Swift model, the HPP model gives rise to anisotropic hydrodynamic equations that are not invariant under a global spatial rotation. At the time, this was not considered a problem, since the real purpose of these models was to study the statistical physics of fluids, and both models could do this well. Traditional computational fluid dynamicists, however, were not inclined to take notice of this as a serious numerical method unless and until a way was found to remove the unphysical anisotropy (Boghosian, 1999). Thirteen years passed from the introduction of the HPP model to the solution of the anisotropy problem in 1986 by Uriel Frisch, Brosl Hasslacher and Yves Pomeau (Frisch et al, 1986), and simultaneously by Stephen Wolfram (Wolfram, 1986). Frisch, Hasslacher and Pomeau demonstrated that it is possible to simulate the Navier-Stokes equations of fluid flows by using a cellular automaton of gas particles on a hexagonal lattice, with extremely simple translation and collision rules governing the movement of the particles. In the FHP model, named after the authors of the first reference given above, all the particles have unit mass and move with the same speed hopping from site to site in a hexagonal two-dimensional lattice. The dynamics of this system involves a set of collision rules such that momentum and particle number are conserved (kinetic energy is trivially conserved). From a strict theoretical point of view, it is not clear at the present time if the lattice gas collective equations are equivalent to the Navier-Stokes equations, or if they include them as a particular case. However, there has been a growing interest in studying the viscous fluid flow using lattice gas models due to its great facility to handle complex boundary and initial conditions, and also because the computer simulations have shown that lattice gases behave like normal fluids under some restricted conditions (Hasslacher, 1987; Salcido & Rechtman, 1991, 1993; Rechtman & Salcido, 1996; Salcido, 1993, 1994). The FHP model, in particular, is now considered as an efficient way to simulate viscous flows at moderate Mach numbers in situations involving complex boundaries. However, it is unable to represent thermal or diffusional effects since all particles have the same speed and are of the same nature (Chen et al., 1989). Maybe the simplest lattice gas with thermal properties is a nine-velocities model defined on a square two-dimensional lattice where particles may be at rest or travelling to their nearest or next nearest neighbours (Chen et al., 1989; Rechtman et al., 1990, 1992; Salcido & Rechtman, 1991, 1993; Rechtman & Salcido, 1996).

One of the first attempts to use a lattice gas as an alternative approach in air pollution modelling applications can be found in the work by A. Salcido (Salcido, 1993, 1994; Salcido et al., 1993). There, it is shown how the lattice gas rules, in spite of their relative simplicity, are sufficient to simulate, at least qualitatively, some complex processes affecting unsteady dispersion, including momentum exchange with the surrounding atmosphere and deposition. More recent attempts are found in the work by A. Sciarretta and R. Cipollone (Sciarretta & Cipollone, 2001, 2002; Sciarretta 2006), where a comprehensive stochastic lattice gas model, which provides also reliable quantitative predictions, is presented.

In this work we describe and apply a two-dimensional (2D) lattice gas approach to estimate the MCMA surface wind field from the hourly meteorological data registered at the stations of the official atmospheric monitoring network. This approach is based on the simplest lattice gas with thermal properties. It is a square lattice gas model with interactions up to

second nearest neighbours that conserve the number of particles, momentum and kinetic energy. Within this framework, the best wind field estimate is given by the steady state lattice gas flow which is consistent with the wind velocity values imposed to a number of control lattice sites representing the positions of the meteorological stations, and with a number of forbidden lattice sites that represent the solid boundaries defined by the MCMA topography. The application to the MCMA study case was carried out for the meteorological conditions which prevailed there during the 1994 summertime. As a first step, a model wind direction state, which reflects in a discrete and simplified way the main features of the complex spatial structure of the surface wind circulation events, is used to obtain the density of states of wind direction of the MCMA, as well as a qualitative and quantitative identification of the main wind circulation patterns for daytime and nighttime hours of the dry and rainy seasons of 1994. This first analysis phase helped us to select the particular (but important) daytime and nighttime MCMA wind circulation events which we considered as study cases for the lattice gas simulation of the respective wind fields. The computer simulations were carried out using wind velocity data obtained during a four-site micrometeorological campaign we carried out in Mexico City during the 1994 summertime. The results were compared against the wind data registered by the stations of the official atmospheric monitoring network of Mexico City. A previous description of these results was reported by A. Salcido, A. T. Celada and T. Castro in 2008 (Salcido et al., 2008).

The rest of this chapter is organized as follows: Section 2 is dedicated to describe the basis of the nine-velocity lattice gas model, its equilibrium theory, and some of the simulations we have carried out to test the hydrodynamic behavior of this model. In Section 3, the lattice gas approach we are proposing for the wind field estimation problem is detailed. In Section 4, the characterization of the MCMA wind circulation events that prevailed there in 1994 is presented in terms of the density of states of wind direction and the main wind circulation patterns that can be identified by means of parameters such as the mean wind direction, the vorticity and the divergence of the MCMA wind direction states. In Section 5, it is described and discussed the application of the lattice gas model in estimating the MCMA wind field for some particular wind circulation events which occurred at both daytime and nighttime hours of the 1994 summertime, as well as the comparison of the simulation results against wind velocity data registered at the stations of the official atmospheric network of Mexico City. Finally, it is included a section devoted to conclusions and suggestions for future work.

2. The Nine-Velocity Lattice Gas Model

We will consider a cellular automaton defined on a square 2D lattice containing N_x times N_y sites. The state at any lattice site \mathbf{r} indicates the presence or absence of particles travelling in nine allowed directions defined by the vectors:

$$\mathbf{e}_\alpha = \begin{cases} 0 & \alpha = 0 \\ \cos\left((\alpha - 1)\frac{\pi}{4}\right)\mathbf{u}_1 + \sin\left((\alpha - 1)\frac{\pi}{4}\right)\mathbf{u}_2 & \alpha = 1, \dots, 8 \end{cases} \quad (1)$$

where \mathbf{u}_1 and \mathbf{u}_2 are unit vectors along the positive directions of X and Y axes, respectively. The time step and the lattice step along the axes are both defined as unit. The allowed particle speeds c_α and kinetic energies ε_α (assuming particles of unit mass) are defined by

$$c_\alpha = \begin{cases} 0 & \alpha = 0 \\ 1 & \alpha = 1,3,5,7 \\ \sqrt{2} & \alpha = 2,4,6,8 \end{cases} \quad (2)$$

$$\varepsilon_\alpha = \frac{c_\alpha^2}{2} = \begin{cases} 0 & \alpha = 0 \\ 1/2 & \alpha = 1,3,5,7 \\ 1 & \alpha = 2,4,6,8 \end{cases} \quad (3)$$

This means that the model only takes into account particle interactions to the nearest and the next nearest neighbours. An exclusion principle is obeyed by the lattice gas particles in the sense that at any site \mathbf{r} and at any time t there can be no more than one particle moving in each of the allowed directions \mathbf{e}_α . This exclusion principle has deep consequences on the collective (or macroscopic) behaviour of the model.

The state $S(\mathbf{r},t)$ at any lattice site \mathbf{r} at any time t is given by a set of nine Boolean fields, $S_\alpha(\mathbf{r},t)$. Each one of these field variables takes the value 1 (0) in the presence (absence) of a particle traveling in direction α at site \mathbf{r} and time t . The time evolution of the model is defined by a set of, at least, three homogeneous local operators, \mathbf{T} , \mathbf{C} and \mathbf{B} , that represent the translation of particles, the collision between particles, and the collision of particles against fixed obstacles or solid boundaries, respectively. Formally, this can be expressed as

$$S(\mathbf{r},t+1) = \mathbf{B} \circ \mathbf{C} \circ \mathbf{T}(\{S(\mathbf{r}',t) \mid \mathbf{r}' \in V_r\}) \quad (4)$$

where V_r denotes the neighborhood of site \mathbf{r} that contains the site itself, and its nearest and next nearest neighbors. As it is illustrated in Figure 2, the translation operator \mathbf{T} explores all the sites in the neighborhood and moves the particles pointing towards the central site to it. These particles form the input state for the collision operator \mathbf{C} and the output is some other state that has the same number of particles, momentum and energy. The nontrivial collisions of two and three particles are shown schematically in Figure 3 where an open circle indicates a particle at rest and each entry represents all its possible rotations. For each entry, any state may be chosen as the input of the collision and the remaining states are the possible outputs. Although Figure 3 shows only the nontrivial two and three particle collisions, the evolution of the automaton takes into account all particle collisions that can occur involving up to 9 particles. The translation and collision operators define the lattice gas microdynamics and are applied synchronously to all the sites of the lattice. The obstacle operator takes into account boundary conditions and the presence of obstacles. A particle that collides with an obstacle may invert its direction (to simulate, on the collective level, a no-slip condition) or may be reflected (to simulate now a slip condition). Other operators can be introduced to simulate effects due to heating or gravitational forcing (Rechtman et al., 1990; Salcido & Rechtman, 1991). The heating operator, for example, attempts to simulate a heat exchange between the system and its surroundings in such a way that the average energy of the system assumes a given value. A simple implementation of the heating operator is as follows. After the action of the translation, collision and obstacle operators a

small percentage of sites is chosen at random, the average energy is calculated and compared with a given energy control value. If the average energy takes a value greater (smaller) than the control energy, a new state is assigned to each of the chosen sites that has the same number of particles but smaller (greater) energy.

In spite of the simplicity of the rules that define the microdynamics of this model, the computer simulations show that at the collective level it behaves very similar to a real gas under certain conditions, but also can have a non classical behavior under other conditions. In the next two subsections, we present first the equilibrium theory of the 9-velocity lattice gas model and later some few computer simulations we carried out to test its hydrodynamic behavior, both qualitatively and quantitatively.

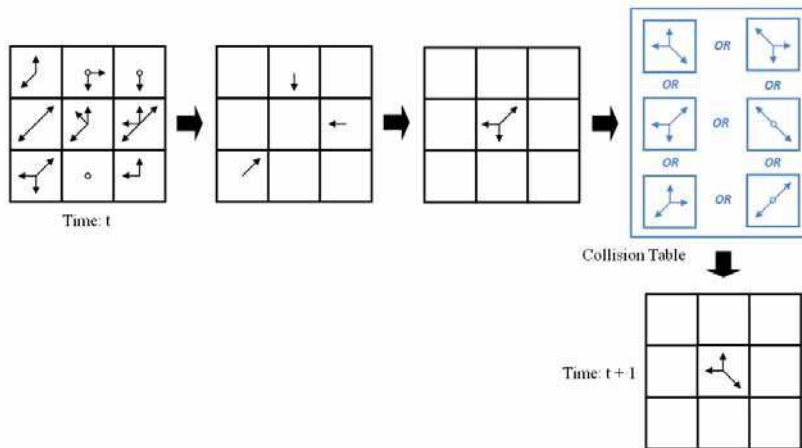


Fig. 2. The propagation and collision of the lattice gas particles.

TWO PARTICLE COLLISIONS	THREE PARTICLE COLLISIONS

Fig. 3. Collisions involving two and three particles.

2.1 Equilibrium Properties

Let n , e and n_α denote the average number of particles per site, the average energy per site, and the average number of particles per site moving in direction \mathbf{e}_α at site \mathbf{r} and at time t , respectively. Then

$$n = \sum_{\alpha} n_{\alpha} \quad (5)$$

$$e = \sum_{\alpha} n_{\alpha} \mathcal{E}_{\alpha} \quad (6)$$

Due to the exclusion principle there are a lower bound (e_{\min}) and an upper bound (e_{\max}) on the energy per site e which depend on the average number of particles per site n as follows:

$$e_{\min} = \begin{cases} 0 & 0 \leq n < 1 \\ \frac{n-1}{2} & 1 \leq n < 5 \\ n-3 & 5 \leq n \leq 9 \end{cases} \quad (7)$$

$$e_{\max} = \begin{cases} n & 0 \leq n < 4 \\ \frac{n+4}{2} & 4 \leq n < 8 \\ 6 & 8 \leq n \leq 9 \end{cases} \quad (8)$$

The graphs of these functions are shown in Figure 4. The area between the two curves represents the set of the allowed states (n, e) of the model.

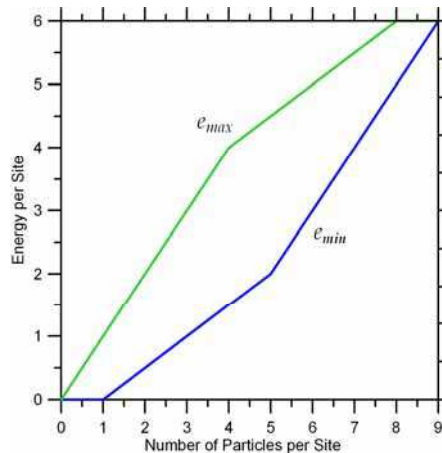


Fig. 4. Minimum and maximum allowed energies.

Now, following the microcanonical equilibrium statistical mechanics, the equilibrium thermodynamic properties can be obtained from the distribution densities \tilde{n}_α that maximize the entropy per site of the system (Salcido & Rechman, 1991)

$$s = -k \sum_{\alpha} [n_{\alpha} \ln n_{\alpha} + (1 - n_{\alpha}) \ln(1 - n_{\alpha})] \quad (9)$$

under the constraints imposed by the equations (5) and (6). In this equation k is the Boltzmann constant, which hereafter will be considered equal to 1, for simplicity. By employing the method of undetermined Lagrange multipliers, the distribution densities \tilde{n}_α of the equilibrium states are obtained:

$$\tilde{n}_{\alpha} = \frac{1}{1 + e^{(a+b\varepsilon_{\alpha})}} \quad (10)$$

where a and b are the Lagrange multipliers. Now, to get some insight about the physical meaning of the Lagrange multipliers a and b , we note that, using equations (10), the entropy can be written as

$$s = an + be - \sum_{\alpha} \ln(1 - \tilde{n}_{\alpha}) \quad (11)$$

Then, a formal comparison of this equation with the well known Euler equation of thermodynamics for a gas of particles,

$$s = -\frac{\mu}{T} n + \frac{1}{T} e + \frac{P}{T} \quad (12)$$

suggests the following thermodynamic-like interpretation:

$$\begin{aligned} a &= -\frac{\mu}{T} \\ b &= \frac{1}{T} \\ \frac{P}{T} &= -\sum_{\alpha} \ln(1 - \tilde{n}_{\alpha}) \end{aligned} \quad (13)$$

In the Euler equation (12), s is the entropy per unit volume, n is the density of the number of particles, T is the temperature, μ is the chemical potential, e is the internal energy per unit volume, and P is the pressure.

Strictly speaking, the first two equations (13) just define the new parameters T and μ in terms of the Lagrange multipliers a and b , and the last one defines P . However, the use of these properties, which we will call temperature (T), chemical potential (μ), and pressure (P)

of the lattice gas, opens a useful framework for the physical analysis and interpretation of lattice gas behavior. In terms of the temperature and chemical potential, the distribution densities \tilde{n}_α of the equilibrium states can be expressed as

$$\tilde{n}_\alpha = \frac{1}{1 + e^{(\varepsilon_\alpha - \mu)/T}} \tag{14}$$

So, at equilibrium the lattice gas particles will organize themselves among the possible velocities according to a Fermi-Dirac distribution. This is a consequence of the exclusion principle that must be obeyed by the lattice gas particles. Under equilibrium conditions, as it is implied also by equation (14), the same number of particles moves along each diagonal direction and also along the vertical and horizontal ones:

$$\tilde{n}_1 = \tilde{n}_3 = \tilde{n}_5 = \tilde{n}_7 \quad \tilde{n}_2 = \tilde{n}_4 = \tilde{n}_6 = \tilde{n}_8 \tag{15}$$

These theoretical results agree with the computer simulations we performed to test the equilibrium properties of the model. We started with a 200×100 sites lattice and particles tossed at random in position and direction of motion keeping the average number of particles per site n fixed. With a heating operator, the lattice gas was cooled or heated for 500 time steps to fix its energy to a given control value and then left to equilibrate for another 500 time steps. Finally the experimental distribution densities were computed. In Figure 5, the plots for the theoretical equilibrium distribution densities $\tilde{n}_0, \tilde{n}_1,$ and $\tilde{n}_2,$ including the corresponding simulation results, are presented for $n = 1$ and $n = 3$. This figure shows also that a population inversion takes place in the high energy limit.

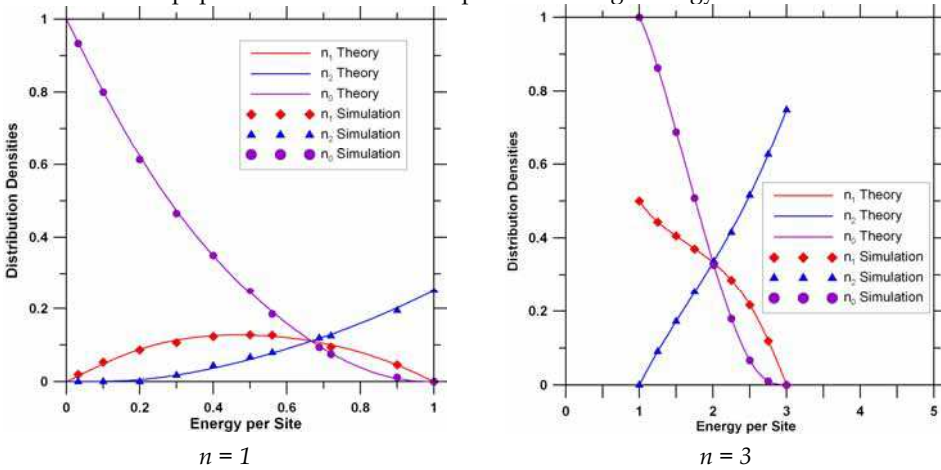


Fig. 5. Comparison of the theoretical and experimental (simulated) equilibrium distribution densities for average numbers of particles $n = 1$ ($e_{min} = 0$ and $e_{max} = 1$) and $n = 3$ ($e_{min} = 1$ and $e_{max} = 3$).

In figures 6, the plots for the entropy per site (Fig. 6a), the temperature (Fig. 6b), the pressure (Fig. 6c), and the chemical potential (Fig. 6d), as functions of the energy per site e , for a number of particles per site $n = 1$, are presented.

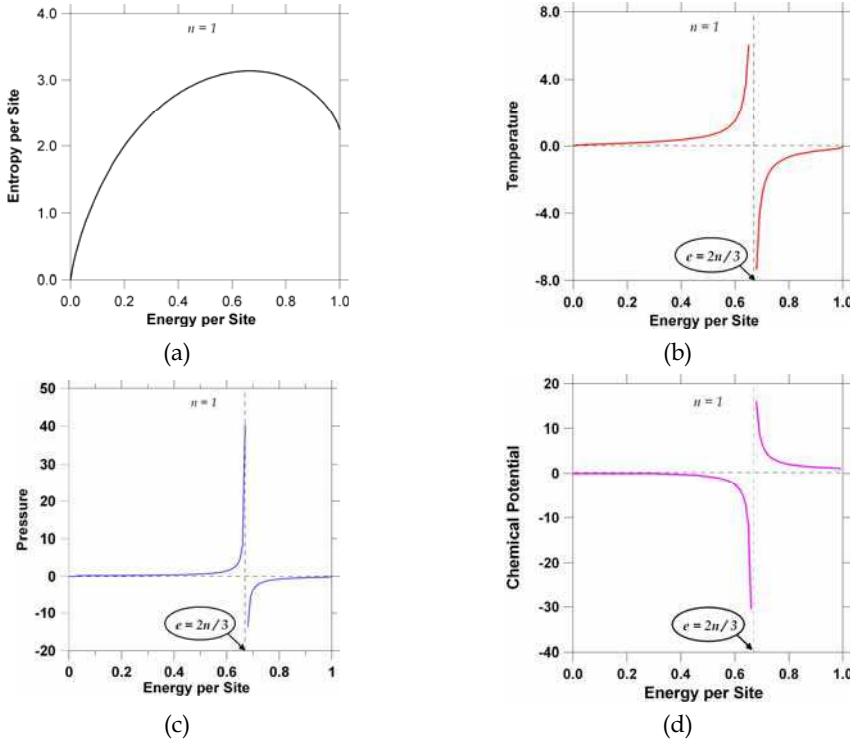


Fig. 6. (a) entropy per site, (b) temperature, (c) pressure, and (d) chemical potential, them all plotted as functions of the energy per site, for $n = 1$.

This figures show that the thermodynamic properties of the lattice gas models have non-classical behaviors. Temperature and pressure, in particular, can assume positive and negative values with an infinite discontinuity at the energy $e = (2/3)n$. This is a consequence of the exclusion principle and of the finite nature of the energy spectrum in these systems. However, it is worth to mention that, in spite of this non classical behavior, for small values of n (that is, in the low density limit) the relation between pressure and temperature can be written as the state equation of an ideal gas:

$$P = -T \sum_{\alpha} \ln(1 - n_{\alpha}) \xrightarrow{n \rightarrow 0} P = nT \tag{16}$$

This result is an indication that, under restricted conditions, the lattice gas may be useful as a model of a classical gas. Other equilibrium thermodynamic properties, such as the specific heat and compressibility, can also be computed from the equilibrium distribution densities.

2.2 Qualitative Hydrodynamic Behavior of the 9-Velocity Lattice Gas

Here we present the results of three different computer simulations we carried out to test the hydrodynamic behavior of the 9-velocity lattice gas model at a qualitative level. The first two simulations show that the model gas behaves as expected in flows past fixed obstacles, and the last one tests the model ability to simulate wave phenomena.

Simulation of flows past fixed obstacles. Figures 7 show the sequences of velocity field sketches obtained from the simulation of the flow past a solid bar (left) and a wedge (right), respectively. A lattice with 300×200 sites was used. No gravity neither heating effects were considered. We imposed a flow by initially putting particles at random in the upwards directions (e_0 , e_1 , and e_2) with an average number of particles per site $n = 2.7$. Particles leaving the top row were introduced in the bottom row randomly but moving upwards. The obstacle operator was defined in the other vertical sides of the lattice and on the obstacle boundary in order to simulate a no-slip condition at the collective level. Both sequences correspond to 2000 time steps of the automaton evolution. Each velocity field was constructed from the experimental distribution functions defined as averages over cells containing 7×7 lattice sites. The left hand sequence shows two vortices opposite to each other growing past a horizontal bar as time proceeds, such as it is expected for this flow for Reynolds numbers within a certain range. Note also the fluid velocity goes to zero on solid boundaries. In the sequence of the flow past the wedge, it is interesting to observe how the presence of solid wall at right side of the channel forces the development of an adjacent vortex although no obstacle is located there. It would not occur if the system could extend infinitely in the horizontal direction.

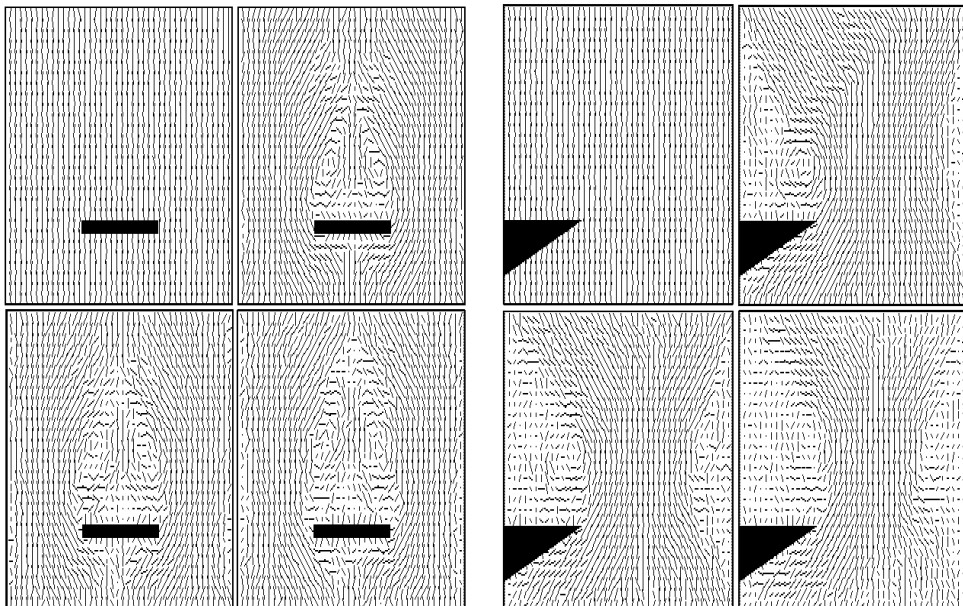


Fig. 7. Lattice gas simulation of the flow past a horizontal bar (left) and a wedge (right), along a vertical channel. No gravity neither heating effects were included.

Simulation of wave phenomena. Figure 8 shows a sequence of the development of a density wave in a closed square box starting from an initial condition where the gas density is uniform everywhere with exception of a centred empty circular hole. A 200×200 sites lattice with periodic boundary conditions was used for the computer simulations and no gravity neither heating effects were considered. The gas particles were tossed at random in position and direction of motion keeping an average number of particles per site $n = 2$. Then all the particles located inside a centered circle of given radius were deleted to simulate an empty hole (that is, an initial density perturbation), and the system was allowed to evolve during a number of time steps that was large enough to record the density wave patterns of a full period, at least. As it can be observed, the sequence of density patterns resembles very strongly the wave phenomena which take place in a real gas system.

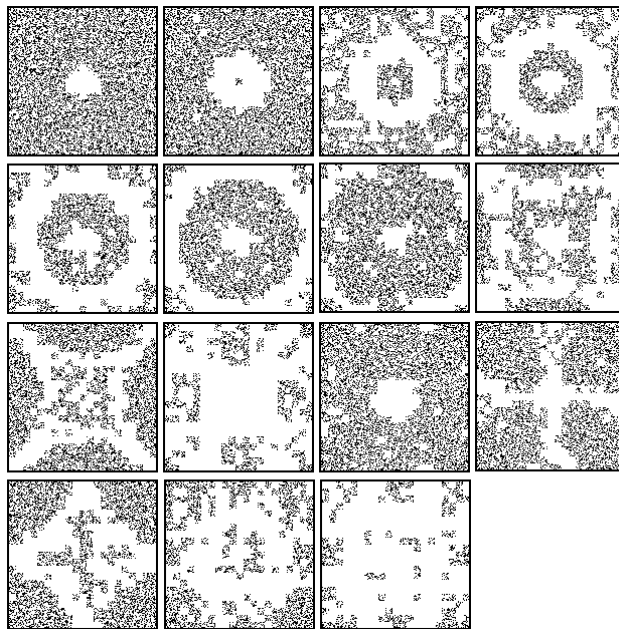


Fig. 8. Lattice gas simulation of a density wave. Initial state: uniform gas with a centred hole (empty) contained in a square box.

2.3 Simulation of Viscous Flows

We have performed two different computer simulations to carry out a simple comparison the 9-velocity lattice gas behaviour against the solutions of the Navier-Stokes equations for the well known Poiseuille and Couette plane flows.

Poiseuille Flow. The steady state flow between two stationary parallel plates driven by an imposed pressure gradient is known as the plane Poiseuille flow. The first simulation we have performed deals with a flow situation more complex than the Poiseuille flow: the relaxation from uniform to equilibrium of the flow between two stationary parallel plates. We used a square lattice with side length $L = 207$ lattice sites. The model gas was contained

between two straight line boundaries at $Y = 0$ (bottom lattice side) and $Y = 207$ (top lattice side). The initial distribution densities were calculated assuming a horizontal flow with uniform velocity $U = 0.15$, an average number of particles per site $n = 2.5$, and an average temperature $T = 10$ (all the magnitudes expressed in the lattice gas units). The obstacle operator \mathbf{B} was implemented for the top and bottom sides of the lattice in order to simulate a flow along a 2D channel with stationary rigid walls. Periodic boundary conditions were imposed on the other two lattice sides, such that no pressure gradient was present along the channel and the evolution of the system was influenced only by the rigid boundaries. The transversal average velocity profiles are shown in Figure 9. Here we can observe, in agreement with the solution of the Navier-Stokes equations for the plane Poiseuille flow, how a parabolic velocity profile decreases with time, indicating dissipation of momentum and energy due to the collisions of the particles each other and with the solid boundaries.

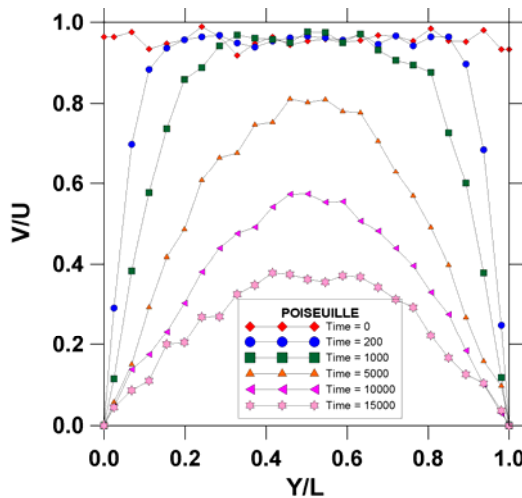


Fig. 9. A non-steady Poiseuille flow. Relaxation from uniform to rest of a 2D flow between two stationary parallel plates.

Couette Flow. The steady state flow between two parallel plates in relative motion is known as the plane Couette flow (see Figure 10 (left)). We performed a lattice gas simulation of the development of a plane Couette flow in two dimensions. A square lattice with side length $L = 207$ lattice sites was considered. The initial distribution densities were calculated by assuming that the gas is initially at rest with an average number of particles per site $n = 2.5$ and an average temperature $T = 10$ (in the lattice gas units). The model gas was contained between two straight line boundaries at $Y = 0$ (top lattice side) and $Y = 207$ (bottom lattice side). The obstacle operator \mathbf{B} was implemented for the bottom side of the lattice in order to simulate a stationary rigid wall. A uniform in average horizontal velocity, $U = 0.15$ (in the lattice gas units), was imposed at the first five top rows of lattice sites to simulate a moving plate. Periodic boundary conditions were imposed on the left and right sides of the lattice (this way, the pressure gradient is zero and that the only forcing on the fluid is forcing due to the moving plate). Ten computer simulations, 15,000 time-steps each, were done with the same initial and boundary conditions. The vertical profiles of average velocity were

obtained for time-steps $t=0, 200, 1000, 5000$ and 15000 . These profiles are shown in Figure 10. It can be observed in this figure how, due to the viscosity of the lattice gas, the relative velocity between the top and bottom boundaries gradually forces the movement of the model gas (initially at rest) with a clear tendency towards a linear profile. The viscosity makes the fluid stick to the boundary which is why a shear develops within the interior of the fluid. The time evolution of the simulated velocity profile and its asymptotical form are in agreement with the solution of the Navier-Stokes equations for the development from rest to the steady state of the laminar viscous flow between two parallel rigid plates in uniform relative motion (Batchelor, 1967).

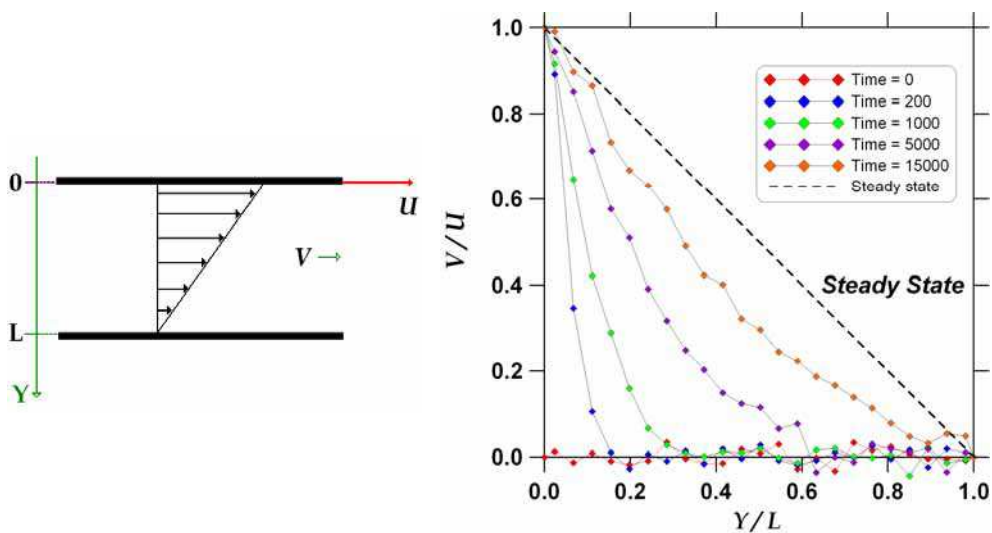


Fig. 10. Simulation of the Couette flow. Development from rest to the steady state.

3. Lattice Gas Simulation of Wind Fields

One of the main attractive features of the fluid flow simulation with lattice gas models is its ability to handle complex initial and boundary conditions. This is one of the reasons why we considered convenient to investigate the lattice gas possibilities as an alternative approach for solving the problems (both diagnosis and prognosis) of the wind fields prevailing in topographically complex terrains.

A simple meteorological outline of the wind field diagnosis problem is as follows: At the stations of an atmospheric monitoring network, the meteorological variables of pressure, temperature, and wind speed and wind direction are measured at a number of sites spatially distributed over a topographically complex and relatively large region. So, for any given time, the meteorological data registered at the network stations are to be used offline to estimate the wind velocity at any given point within the spatial domain of interest.

Within the framework of the computational fluid dynamics, the approach to the problem is focused on solving numerically the set of balance differential equations to find out the steady state of the system that complies the constraints imposed by the boundary (complex topography) and time asymptotic (measured values) conditions. Otherwise, in the lattice gas

approach to the wind field estimation problem, the available data of pressure, temperature and wind velocity are used to compute the steady state distribution functions, $n_\alpha(\mathbf{r}_i)$, for a given number of control lattice sites \mathbf{r}_i . The topographic data, on another hand, are used to define some special domains of lattice sites which are to be forbidden to the particles of the model gas; these particular domains are defined in order to represent the fixed obstacles in the computer simulations, and the obstacle operator will affect the particles arriving to their boundaries. Once the system has been prepared, it is allowed to evolve during a given number of time steps. The number of time steps that the system requires to reach a steady state depends on the size of the lattice and on the number of control points it comprises.

Under equilibrium conditions, the values of the distribution functions at the control points can be computed using the equilibrium formalism of the section 2.1 after an appropriate scaling procedure to express the meteorological data in the lattice gas units. Out of equilibrium, the same approach can be used by assuming local equilibrium conditions and using a constrained perturbation technique in order to satisfy the desired local velocity conditions for a given number of particles per site n . So,

$$n_\alpha = \tilde{n}_\alpha + \delta n_\alpha, \quad \sum_\alpha \delta n_\alpha = 0, \quad \mathbf{v}(\mathbf{r}, t) = \frac{1}{n} \sum_\alpha c_\alpha \mathbf{e}_\alpha \delta n_\alpha \quad (17)$$

The outputs of the computer simulations are average distribution functions computed over cells of 9×9 lattice sites. While the simulation goes on, the average distribution densities, denoted as $f_\alpha(\mathbf{x}, t)$, can be computed as frequently as it is desired for each cell position \mathbf{x} , and they are used to calculate the wind velocity $\mathbf{v}(\mathbf{x}, t)$ as follows:

$$\mathbf{v}(\mathbf{x}, t) = \frac{1}{f} \sum_\alpha c_\alpha \mathbf{e}_\alpha f_\alpha(\mathbf{x}, t), \quad f(\mathbf{x}, t) = \sum_\alpha f_\alpha(\mathbf{x}, t) \quad (18)$$

Before considering a real and practical study case, a few computer simulations were carried out to test the lattice gas capabilities in modelling of situations of turbulent flow similar to those ones which prevail in the atmospheric surface layer. Our main concern was to find out the ability of the model to reproduce the well known quasi-logarithmic wind velocity profile

$$u(y) = \frac{u_*}{\kappa} \left[\ln \left(\frac{y}{y_0} \right) - \Psi_M \left(\frac{y}{L} \right) \right] \quad (19)$$

where u is the mean wind velocity, u_* is the friction velocity, κ is the von Karman constant, y is the height over the earth surface, y_0 is the roughness length, L is the Monin-Obukhov length, and Ψ_M is a universal function which takes into account corrections to the logarithmic profile due to the atmospheric stability conditions (Garrat, 1992).

The computer simulations were performed with a lattice that comprised 207×207 sites. Periodic boundary conditions were imposed on the left and right sides of the lattice. The bottom side ($y = 0$) was filled with small obstacle towers whose heights were chosen randomly to simulate a roughness length equal to 5 % of the lattice side length ($y_0 \sim 10.35$).

The lattice gas was assumed initially at rest on the average, with a number of particles per site $n = 2.5$, and a temperature $T = 10$. In the top lattice side ($y = 207$) it was imposed a fixed horizontal velocity U using the first five lattice rows as control points. Ten computer simulations, 35000 time steps each one, were made for $U = 0.1, 0.3, 0.5, 0.7$ and 0.9 with the same initial and boundary conditions. In Figure 11 there are shown the mean wind velocity profiles obtained for $U = 0.3$ and times $t = 0, 1000, 5000, 10000, 20000, 25000, 30000$ and 35000 . In this figure we note that the system reached the steady state flow conditions (continuous straight line), that the steady state velocity profile is linear such as it is predicted by the Navier-Stokes equations in the laminar case (Batchelor, 1967), and that, because the roughness of the bottom lattice side, the wind velocity became zero near (but not at) the surface ($V/U \sim 0$ at $Y/L \sim 0.058$).

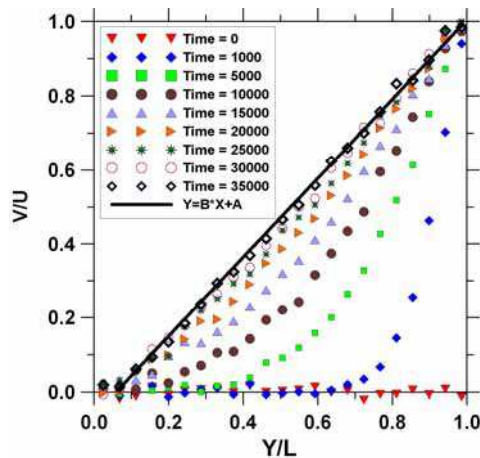


Fig. 11. Lattice gas simulation of the Couette flow development from rest to the steady state, when a no null roughness length is associated to the bottom stationary plate.

In figure 12 there are shown the wind velocity profiles for $t = 35000$ and $U = 0.1, 0.3, 0.5, 0.7$ and 0.9 , and it can be observed that the velocity profile deviates from the linear case as U increases. This is what really happens on the transition of the flow from a laminar state to a turbulent one. For $U = 0.9$ the velocity profile is, in fact, quasi-logarithmic. In this figure, the solid curve corresponds to the equation (19) with $u^*/k = 0.3$ and Ψ_M given by

$$\Psi_M = a(y - y_0) \ln \left(\frac{y + 1}{b(y - 1)} \right) \tag{20}$$

where $y_0 = 10.5$, $a = 0.2$ and $b = 1.016$. Although the 9-velocity lattice gas model may have a clearly non-classical behaviour at energies higher than $2n/3$, the results of the various simulations that we have performed show that it can be useful for some meteorological applications, such as the wind field estimation problem, if it is handled carefully. The ranges of values of the density and the energy which are safe for a particular practical application might be identified previously.

Thank You for previewing this eBook

You can read the full version of this eBook in different formats:

- HTML (Free /Available to everyone)
- PDF / TXT (Available to V.I.P. members. Free Standard members can access up to 5 PDF/TXT eBooks per month each month)
- Epub & Mobipocket (Exclusive to V.I.P. members)

To download this full book, simply select the format you desire below

